LAWRENCE
LIVERMORE
NATIONAL
LABORATORY

LLNL-TR-582223

Soil Composition, Area 6 of the Nevada National Security Site

K. B. Knight, R. Albo, G. Eppich, S. Roberts, M. Singleton

Lawrence Livermore National Laboratory

September 2012

Disclaimer

Auspices Statement

This work performed under the auspices of the U.S. Department of Energy by Lawrence Livermore National Laboratory under Contract DE-AC52-07NA27344.

Soil Composition, Area 6

Three soil samples (two from the surrounding soils and one from the intersecting gravel roadbed) were collected from Frenchman Flat Area 6, across from the DAF at the Nevada National Security Site for analysis of major and trace element compositions.

Table 1: Samples

Sample	Origin
A	Area 6 soil
B	Area 6 soil
C	Area 6 roadbed

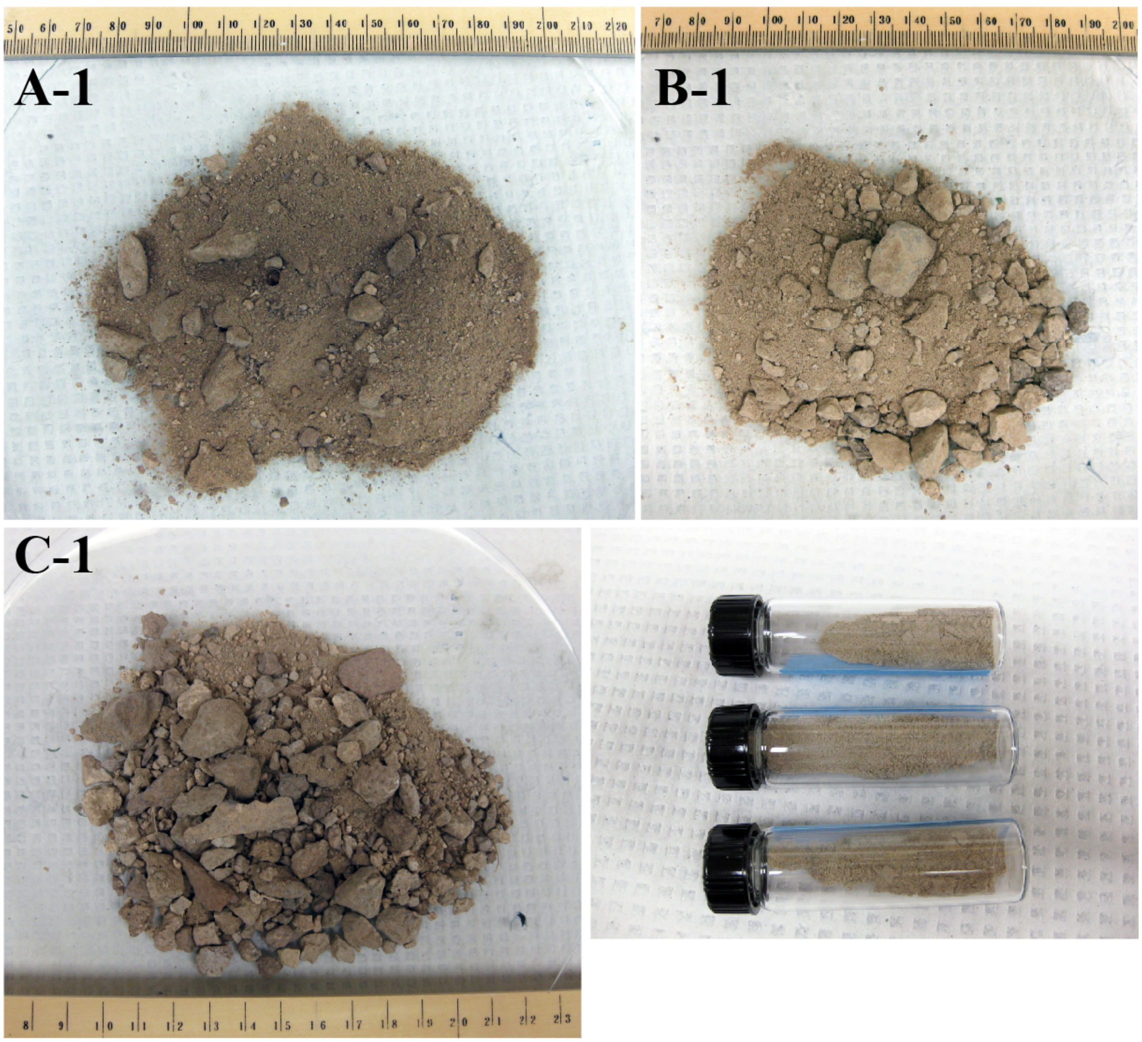

Figure 1: Raw (as provided) and crushed (vials) soil samples

Sub-samples were homogenized into a powder in an agate mortar. Aliquots were then distributed for various types of analysis. A summary of these analyses are given below:

Table 2: Analytical Techniques

Technique	Elements
Mineral Analysis by Powder Diffraction (XRD)	Major mineral phases
Light element combustion analysis	C, H, N, O, S
X-ray fluorescence (XRF)	Major and trace elements
Plasma Mass Spectrometry (ICP-MS)	Major and trace elements

Mineral Analysis by Powder Diffraction

X-ray powder diffraction (XRD) is a rapid analytical technique primarily used for phase identification of a crystalline material based on constructive interference of monochromatic X-rays and a crystalline sample. The analyzed material is finely ground, homogenized, and average bulk composition is determined. X-ray powder diffraction is most widely used for the identification of unknown crystalline materials (e.g. minerals, inorganic compounds).

For these soils, powdered samples were analyzed on a Bruker AXS D8 ADVANCE X-ray diffractometer equipped with a LynxEye 1-dimentional linear Si strip detector. DIFFRACplus Evaluation package Release 2009 software was used for the data analysis. The unknown samples were scanned from 5-75° 2θ. The step scan parameters were 0.02° step and 2 second counting time per step with a 15mm variable divergence slit and a 1.0° antiscatter slit. The samples were x-rayed with Ni-filter Cu radiation from a sealed tube operated at 40kV and 40mA. Phases in the unknown samples were identified by comparison of observed peaks to those in the International Centre for Diffraction Data (ICDD PDF2009) powder diffraction database. X-ray reference material (Bruker supplied Al_2O_3) was analyzed during the time of the unknown runs to ensure goniometer alignment. No peak shift was observed in the reference material.

Table 3: XRD results

Sample	Major phase	Minor phases
A1	Quartz	Na-, Ca-, and K- feldspar, minor amounts of iron and clay
B1	Quartz	Na-, Ca-, and K- feldspar, minor amounts of iron and clay
C1	Quartz	Na-, Ca-, and K- feldspar, minor amounts of iron and clay

XRD scans revealed similar mineralogy for all three samples (the two soils as well as the road bed sample), with quartz (SiO_2) as the major mineral phase. Feldspar minerals ($KAlSi_3O_8$-$NaAlSi_3O_8$-$CaAl_2Si_2O_8$) were the dominant minor constituents. Sample C contained significant Albite (Ca-feldspar) absent in the other two samples.

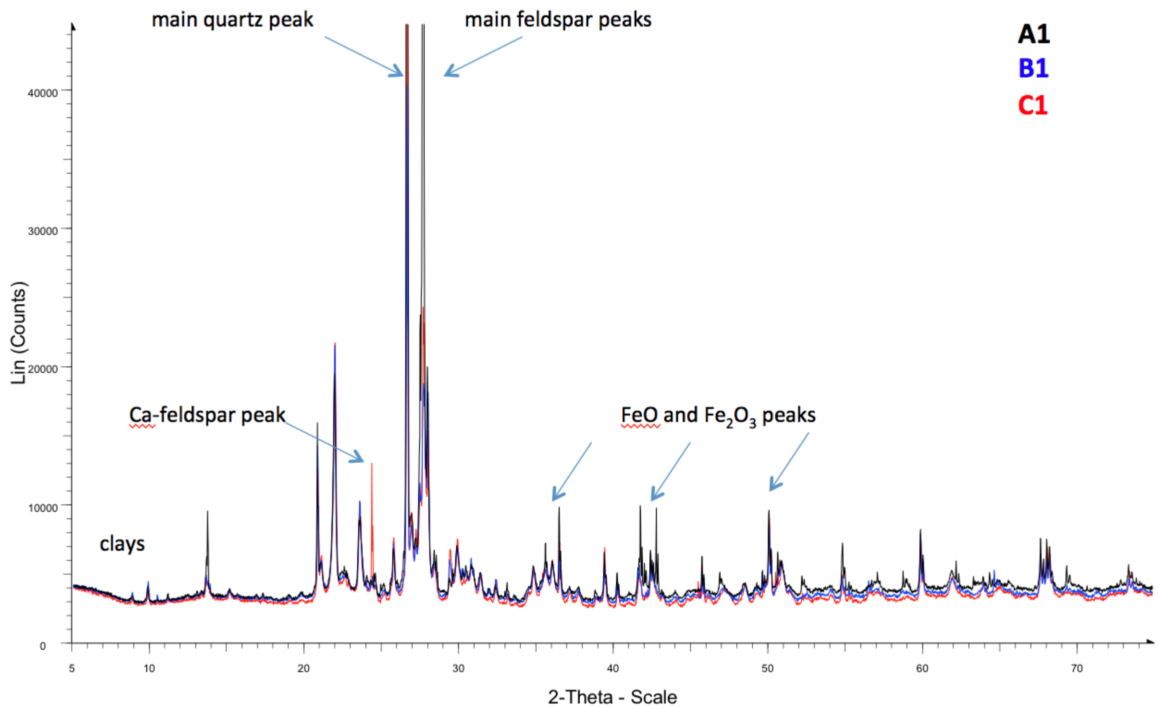

Figure 2: X-ray diffraction scans of the three samples (not background subtracted) showing the similarities in diffraction patterns and mineralogical composition.

Light Element Combustion Analyses

The carbon and nitrogen analysis was performed using the EA 1100 Elemental Analyzer (CE Instruments). This is an automated dry combustion system utilizing high-temperature combustion (oxidation) of the sample, followed by use of a carrier gas system to move the oxidized products through the system to the analyzer.

A sulfanilamide standard was used to prepare the linear calibration curve for the 2 elements. Approximately 20 mg of soil from each sample was loaded into tin capsules for analysis, each soil analyzed in triplicate. Samples were combusted in a column held at 920˚C consisting of WO_3 and copper. When the sample is dropped into the combustion tube, the exothermic Sn combustion reaction reaches 1700˚C. A gas chromatography system traps and separates the detected gases followed by detection by a TCD (thermal conductivity detector), with C determined as CO_2 and N as N_2.

For S determinations, solid samples were loaded into tin capsules, and weighed out on a Mettler Toledo XP2U microbalance with elemental compositions determined using an Elementar Vario PyroCube EA. Samples dropped into the EA were combusted at 1020° C over tungsten oxide in a continuous stream of helium carrier gas to produce SO_3 from any sulfur present in the sample. The resulting gas then passed through a reduced copper reactor at 650° C to reduce SO_3 to SO_2, and trap any volatile halogen compounds on silver wool. Following water removal using a Sicapent adsorption tube, the SO_2 analyte gases were separated and purified using purge-trap columns, and then carried through a thermal conductivity detector (TCD). The TCD signal is passed to computer software that calculates elemental abundances based on integrated TCD peak areas.

For S analyses, we ran samples A1 and B1 once, and sample C1 in duplicate as a check for consistency. C was also determined as CO_2 by this method. This yielded results entirely consistent with those from the above CN analyses, but with larger errors resulting from the smaller sample size, and is thus not reported, here. Lower limits for quantification and errors were determined by running 3 concentration standards containing the elements of interest and 3 blank samples will be run prior to analyzing samples.

To measure oxygen concentrations, powdered samples were loaded into Ni crucibles. This procedure then uses a reaction with chlorine trifluoride (ClF_3) to convert oxygen from silicate and oxide materials into oxygen gas (O_2). The O_2 is subsequently converted to carbon dioxide gas (CO_2), and yield is measured using a manometer. The use of high vacuum fluorination systems to extract oxygen from silicate and other oxide phases using halogen fluorides or fluorine gas is well documented in peer-reviewed literature. The typical uncertainty for runs in this laboratory is quoted here (± 0.2%).

Table 4: Organic Composition Results

Sample	%N	1 sd	%C	1 sd	% O	1 sd	%S
A1	0.0126	0.0005	0.148	0.011	51.77	0.20	<0.06
B1	0.0189	0.0126	0.294	0.027	45.63	0.20	<0.06
C1	0.0041	0.0005	0.220	0.033	47.74	0.20	<0.06

Values are given as an elemental percent. Errors are the standard deviation from the triplicate analyses for C and N, where variance for all samples and analyses was 0.1% or less. O errors are typical uncertainties. S concentrations were below detection limits (0.0006 g/g) for all samples.

Non-Destructive Major and Trace Element Analyses

Aliquots of powders from each of the three samples were analyzed by X-ray fluorescence (XRF) spectrometry, which is used for routine, relatively non-destructive chemical analyses of rocks, minerals, sediments and fluids. XRF bombards the sample with high-energy X-rays, causing the emission of characteristic "secondary" (or fluorescent) X-rays from elements higher in atomic number than Be (although, in practice, only X-rays from elements higher in atomic number than Na are detected). XRF often provides complementary information to that provided by ICP-MS (see ICP-MS data, below and Tables 7 and 8).

Whole-rock samples were analyzed for element concentrations using a Bruker S8 WD-XRF. Analyses were performed on powdered samples in a helium atmosphere using the Bruker QuantExpress analytical program. The instrument calibration was performed by measuring standard silicate glass discs (Breitländer GmbH), certified for a suite of major and trace elements, under the same operating conditions as the samples. All elements from Na to U were analyzed; only elements measured above detection limits (Table 5)

Table 5: XRF trace and major element results

Oxide	Z	A1	1σ (%)	LLD (ppm)	B1	1σ (%)	LLD (ppm)	C1	1σ (%)	LLD (ppm)
Na_2O	11	**1.14%**	4.47	300.1	**1.05%**	4.91	330.0	**1.33%**	4.18	297.2
MgO	12	**1.59%**	1.75	198.9	**1.63%**	1.75	193.3	**0.96%**	2.39	187.7
Al_2O_3	13	**13.25%**	0.52	118.8	**12.80%**	0.54	115.4	**12.05%**	0.56	112.9
SiO_2	14	**67.90%**	0.21	133.5	**66.23%**	0.22	125.0	**68.24%**	0.22	135.2
P_2O_5	15	**0.23%**	4.32	109.6	**0.21%**	4.60	104.9	**0.16%**	5.37	100.2
SO_3	16	**0.06%**	7.72	74.1	**0.06%**	7.54	73.2	**0.04%**	9.20	71.7
Cl	17	**0.03%**	9.09	53.6	**nd**	25.90	50.1	**nd**	23.90	51.5
K_2O	19	**6.18%**	0.34	40.2	**6.60%**	0.33	39.0	**7.25%**	0.32	41.2
CaO	20	**4.29%**	0.44	92.0	**6.08%**	0.38	96.1	**6.30%**	0.38	101.1
TiO_2	22	**0.71%**	1.06	55.1	**0.73%**	1.09	57.2	**0.47%**	1.39	57.7
Cr_2O_3	24	**68 ppm**	19.00	32.5	**nd**	71.70	34.2	**nd**	42.50	34.2
MnO	25	**0.14%**	1.35	25.5	**0.14%**	1.41	24.7	**0.13%**	1.51	24.2
Fe_2O_3	26	**4.18%**	0.20	82.2	**4.19%**	0.20	83.9	**2.82%**	0.25	22.8
NiO	28	**nd**	34.30	15.4	**54 ppm**	11.30	16.0	**39 ppm**	15.30	15.1
CuO	29	**59 ppm**	8.80	13.1	**50 ppm**	10.80	13.4	**53 ppm**	10.10	13.2
ZnO	30	**0.01%**	3.45	11.6	**0.02%**	3.36	11.9	**0.01%**	4.40	11.6
Ga_2O_3	31	**43 ppm**	10.10	12.5	**40 ppm**	11.50	12.9	**51 ppm**	9.12	12.1
As_2O_3	33	**nd**	9.70	16.1	**nd**	10.30	16.5	**47 ppm**	8.71	10.3
Rb_2O	37	**0.03%**	1.04	8.0	**0.03%**	1.11	8.2	**0.04%**	1.00	8.0
SrO	38	**0.05%**	0.81	7.1	**0.05%**	0.87	7.4	**0.03%**	1.18	7.3
Y_2O_3	39	**5 ppm**	2.60	14.8	**10 ppm**	2.65	15.2	**nd**	2.57	15.6
ZrO_2	40	**0.08%**	0.76	14.8	**0.08%**	0.84	15.2	**0.07%**	1.00	13.8
Nb_2O_5	41	**50 ppm**	6.27	9.4	**36 ppm**	8.85	9.9	**44 ppm**	7.71	9.6
BaO	56	**0.09%**	5.79	176.5	**0.10%**	5.46	182.9	**0.08%**	6.72	172.2
CeO_2	58	**0.02%**	7.83	273.5	**nd**	22.00	290.0	**nd**	12.20	280.2
PbO	82	**51 ppm**	15.80	21.7	**48 ppm**	17.80	22.3	**nd**	54.40	22.4

Sample concentrations are given as weight percent oxides (%), or as parts-per-million by weight (ppm). To convert, for example, 0.09% = 900 ppm, in these units. The lower limits of detection (LLD) are calculated for each sample in ppm. A list of oxides that were not detected in any of the three samples, and their detection limits, is provided in Table 6.

Table 6: Elements and oxides not detected by XRF

Element or Oxide	Z	Average LLD (ppm)	Element or Oxide	Z	Average LLD (ppm)
Sc_2O_3	21	49.5	**Sm_2O_3**	62	88.5
V_2O_5	23	84.6	**Eu_2O_3**	63	141.0
CoO	27	33.2	**Gd_2O_3**	64	70.1
GeO_2	32	11.2	**Tb_4O_7**	65	121.2
SeO_2	34	17.5	**Dy_2O_3**	66	154.3
Br	35	9.1	**Ho_2O_3**	67	49.1
MoO_3	42	13.5	**Er_2O_3**	68	45.9
Ru	44	17.5	**Yb_2O_3**	70	59.3
Rh	45	18.4	**HfO_2**	72	51.4
Pd	46	19.7	**Ta_2O_5**	73	41.0
Ag	47	19.9	**WO_3**	74	38.0
CdO	48	23.4	**Re**	75	69.7
In_2O_3	49	27.2	**Ir**	77	31.9
SnO_2	50	38.3	**Pt**	78	25.2
Sb_2O_3	51	38.9	**Au**	79	23.8
TeO_2	52	65.3	**Hg**	80	23.1
I	53	58.8	**Tl**	81	31.7
Cs_2O	55	92.5	**Bi_2O_3**	83	20.0
La_2O3	57	110.2	**ThO_2**	90	26.5
Pr_6O_{11}	59	96.4	**UO_2**	92	23.4
Nd_2O_3	60	112.5			

Numbers represent the average lower detection limit for each element or oxide species as calculated as the average lower limit of detection (LLD) for each sample calculated as parts-per-million by weight (ppm).

are reported. Table 6 lists elements analyzed for but not detected above detection limits, which were typically on the order of 50-200 ppm. Due to the fact that samples were analyzed non-destructively as loose powders, typical analytical sum totals were ~50 %. Results are reported as oxides, assuming stoichiometric relationships, normalized to 100% totals.

Destructive Major and Trace Element Analyses

Aliquots of the solution intended for trace elemental analysis were diluted in a HNO_3/HF solution to elemental concentrations of ~200 ppm and were then analyzed on a Thermo Electron X7 Quadrupole Inductively Coupled Mass Spectrometer. An internal standard corrects for instrument drift and suppression from the matrix. The results are summarized in the Tables 7 and 8. Major element concentrations are given as elemental weight percent. Trace element concentrations are shown in parts-per-million by weight (micrograms/gram of sample) along with the calculated uncertainties. Masses were calculated from powders as received, with no additional drying.

Table 7: ICP-MS major element results

wt% major element	Z	A1	± 1σ	B1	± 1σ	C1	± 1σ
Na	11	1.856	0.081	1.858	0.068	2.128	0.106
Mg	12	0.611	0.014	0.508	0.012	0.301	0.013
Al	13	6.048	0.111	5.821	0.136	5.696	0.180
K	19	2.904	0.032	3.032	0.111	3.263	0.092
Ca	20	1.253	0.024	1.490	0.047	1.254	0.029
Ti	22	0.186	0.002	0.154	0.003	0.099	0.003
Cr	24	0.002	0.000	0.002	0.000	0.001	0.000
Mn	25	0.052	0.000	0.048	0.001	0.042	0.001
Fe	26	1.337	0.027	1.118	0.022	0.755	0.016

All three samples show very similar major element chemistry, with sample A1 and B1 more closely overlapping than sample C1. The largest major element variations are in the elemental iron content of the samples (~50%). Si (calculated as SiO_2) variations are comparatively minor (see XRF data, Table 5). 51 trace elements were also detected above backgrounds. Trace element data also yield extremely similar chemical compositions, with sample A1 and B1 more closely overlapping than sample C1.

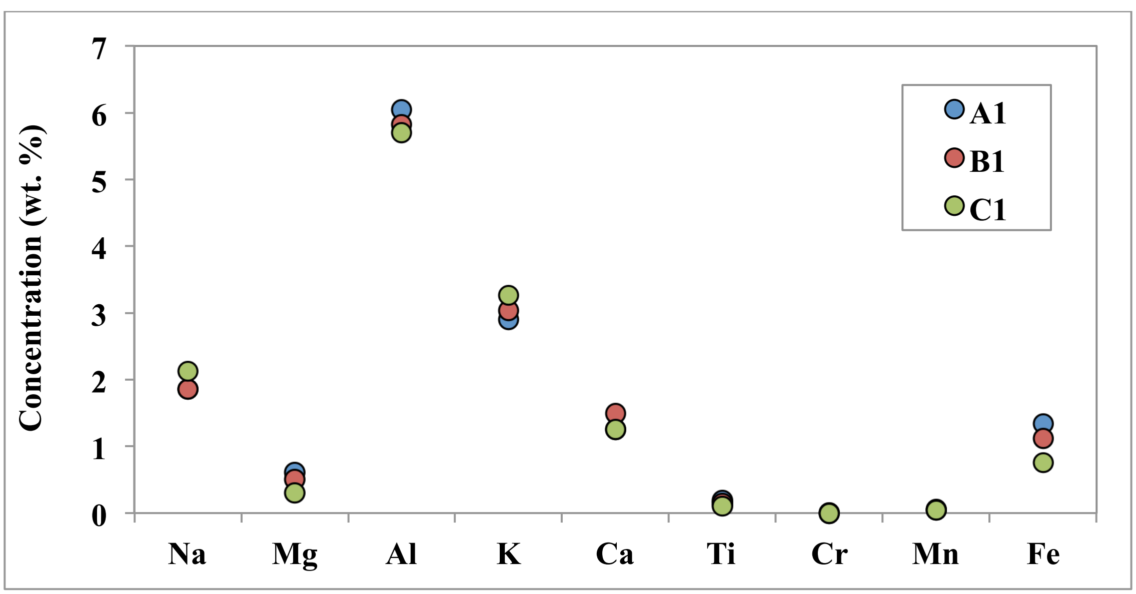

Figure 3: The major element concentrations for the three soil samples. Error bars are smaller than the symbols.

Table 8: ICP-MS trace element results

Trace elements ppm-w	Z	A1	± 1σ	B1	± 1σ	C1	± 1σ
Be	4	2.819	0.192	2.818	0.106	2.926	0.301
V	23	98.112	5.860	71.957	1.594	56.282	1.382
Co	27	3.459	0.090	2.689	0.084	1.227	0.055
Ni	28	6.753	0.349	5.033	0.207	2.161	0.189
Cu	29	7.085	0.203	5.457	0.126	2.782	0.126
Zn	30	50.691	1.485	45.965	2.054	36.694	0.804
Ga	31	15.977	0.248	15.038	0.472	14.338	0.271
Ge	32	8.298	1.116	6.400	0.839	5.676	0.781
As	33	5.337	0.475	4.975	0.445	4.099	0.457
Se	34	0.633	0.143	0.709	0.188	0.483	0.122
Rb	37	137.300	1.521	131.358	3.855	142.766	3.057
Sr	38	187.787	1.209	166.179	4.259	96.589	1.535
Y	39	21.580	0.426	24.646	0.831	21.542	0.416
Zr	40	71.542	0.795	69.320	5.265	70.603	6.479
Nb	41	18.751	0.230	18.518	0.479	18.064	0.444
Mo	42	1.264	0.085	1.063	0.100	1.124	0.073
Ru	44	0.002	0.003	0.001	0.001	0.001	0.003
Rh	45	0.003	0.002	0.002	0.001	0.001	0.001
Pd	46	0.513	0.039	0.589	0.073	0.501	0.056
Ag	47	0.219	0.033	0.194	0.013	0.188	0.016
Cd	48	0.130	0.031	0.127	0.019	0.085	0.018
Sn	50	1.827	0.054	1.775	0.059	1.799	0.236
Sb	51	0.584	0.045	0.486	0.028	0.426	0.030
Te	52	0.034	0.065	0.011	0.014	0.016	0.029
Cs	55	3.662	0.080	3.216	0.054	2.939	0.051
Ba	56	367.505	5.933	327.415	8.594	218.961	3.672
La	57	36.659	0.617	35.706	0.689	35.264	0.663
Ce	58	71.480	1.948	70.414	1.531	69.613	1.687
Pr	59	8.275	0.082	8.220	0.335	7.934	0.203
Nd	60	28.976	0.152	28.780	0.982	27.388	0.617
Sm	62	5.226	0.081	5.354	0.351	5.028	0.115
Eu	63	0.702	0.025	0.684	0.012	0.516	0.021
Gd	64	4.869	0.081	5.094	0.258	4.702	0.181
Tb	65	0.694	0.030	0.740	0.025	0.683	0.028
Dy	66	3.994	0.148	4.401	0.132	3.943	0.038
Ho	67	0.760	0.015	0.857	0.046	0.765	0.016
Er	68	2.351	0.142	2.605	0.057	2.302	0.050
Tm	69	0.332	0.022	0.366	0.012	0.332	0.018
Yb	70	2.242	0.034	2.441	0.065	2.241	0.051

Table 8: ICP-MS trace element results, continued

Trace elements ppm-w	Z	A1	± 1σ	B1	± 1σ	C1	± 1σ
Lu	71	0.323	0.008	0.355	0.019	0.321	0.013
Hf	72	2.822	0.154	2.635	0.127	2.666	0.145
Ta	73	1.802	0.105	1.739	0.147	1.841	0.160
W	74	1.525	0.059	1.439	0.068	1.293	0.043
Re	75	0.003	0.004	0.003	0.001	0.003	0.001
Ir	77	0.011	0.004	0.011	0.004	0.011	0.003
Pt	78	0.027	0.003	0.029	0.008	0.029	0.012
Au	79	0.240	0.040	0.191	0.022	0.176	0.018
Tl	81	0.794	0.029	0.741	0.031	0.795	0.031
Pb	82	22.254	0.162	21.738	0.781	20.872	0.150
Th	90	15.469	0.436	15.893	0.775	16.935	0.618
U	92	3.169	0.044	3.238	0.113	3.188	0.040

Summary

All three samples, while quite distinct in character from other locations at the National Nuclear Security Site, are similar to one another even in the case of the roadbed materials. This suggests that the roadbed material was derived nearby, and does not significantly alter the chemical makeup of the surrounding area. There may be minor differences in density between the nearby soils compared with the roadbed, however, depending on how the road was constructed.

The total water content (not measured here), and corresponding H and O concentrations, will likely vary with season due the presence of clays and weathered minerals in these soils. Composition-based calculations based on these data might consider changing the concentration of H_2O from 0.2 to 5.0% by weight (a reasonable range of water contents), to understand the importance of this effect.

Where non-destructive XRF and dissolution-based ICP-MS overlap, reporting measurements of the same elements, the overlap is in good agreement. For calculation purposes, however, ICP-MS data are to be preferred, as they are based on assumptions of normal isotopic abundances, rather than stoichiometric relationships, and tend to be better quantified (smaller and better characterized errors).

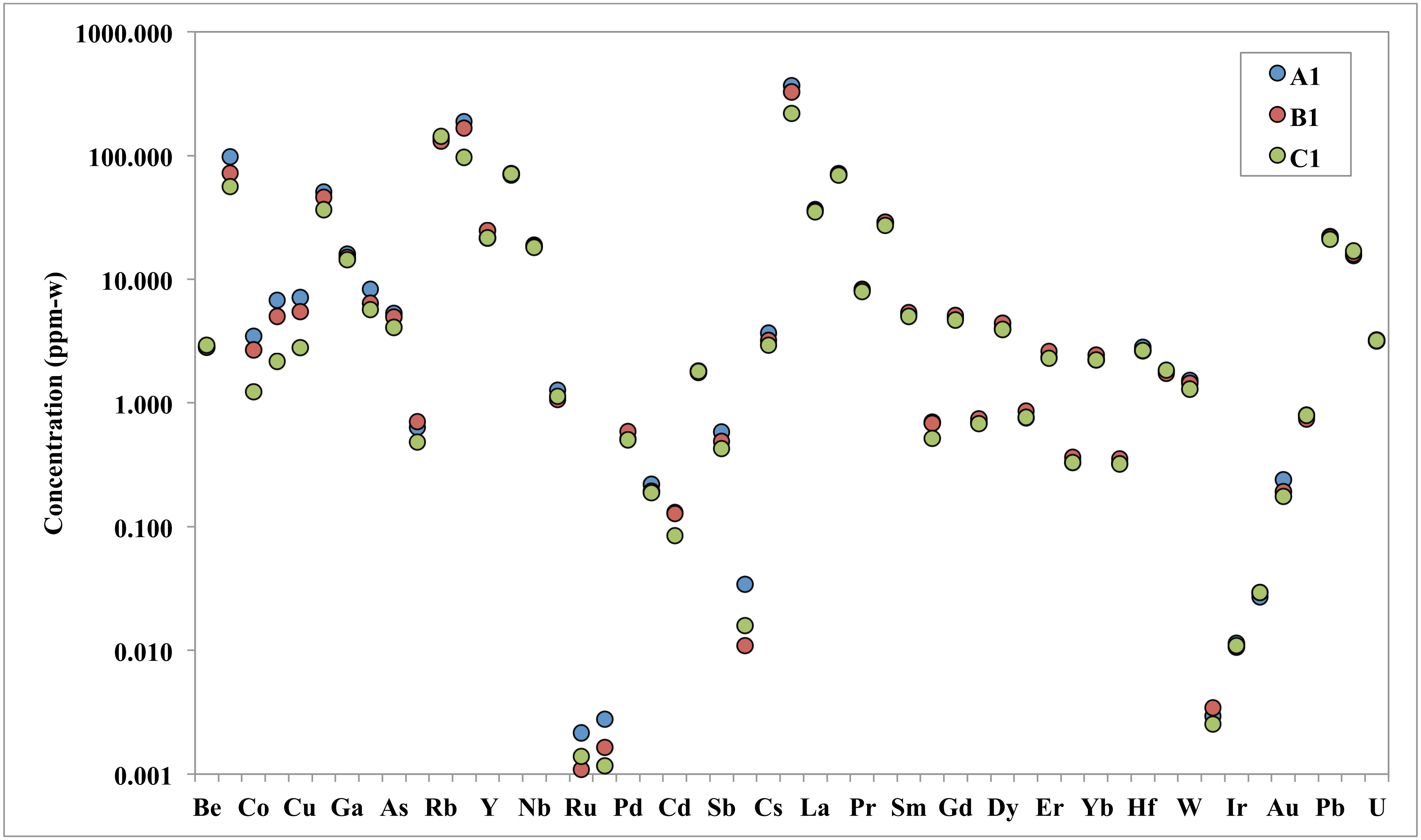

Figure 4: Trace element concentrations for the three soil samples. Error bars are smaller than the symbols.